VII International Conference on Computational Plasticity
COMPLAS 2003
E. Oñate and D.R.J. Owen (Eds)

NUMERICAL SHEAR TESTS FOR DIFFERENT ELASTO-PLASTIC LAWS – COMPLAS 2003

Pierre de Montleau*, Laurent Duchêne, Paulo Flores and Anne-Marie Habraken

*University of Liège, Département MSM
Bâtiment B52/3, 1 chemin des Chevreuils,
4000 Liège 1, Belgium
e-mail: p.demontleau@ulg.ac.be, web page: http://www.ulg.ac.be/matstruc

Key words: kinematic and isotropic hardening, simple shear tests.

Abstract. *This paper presents the numerical simulation of a cyclic simple shear test. The blank tested is a high strength steel sheet for which we use three different constitutive plastic laws derived from Teodosiu's model. These laws take into account respectively isotropic, kinematic and mixed isotropic-kinematic hardening. The goal of the paper is to provide a first numerical idea of the stress-strain path in the center of an experimental test sample.*

1 INTRODUCTION

The industrial requirements (aerospace, car manufacturing) of lighter parts with high mechanical resistance, and at the same time high geometrical accuracy, have motivated the study of metals such as high strength steel and aluminium alloys, and their appropriate forming process. Forming process involves large strains and severe strain-path changing and following its modelisation requires complex laws including anisotropy, isotropic and kinematic hardening as well as texture evolution.
Several essays can be found in literature in order to describe the initial yield locus and to find parameters required by the hardening laws (for example [12]). Taking as a model the essay machine designed at University of Twente [13], a bi-axial test machine is being constructed in the Solid Mechanics Laboratory of the University of Liege. This machine is able to carry out a plane strain test, shear test (monotonic and cyclic) and a simultaneously combination of both, which is very practical when orthogonal path changing is being studied. In this article, we focus on cyclic shear test and reverse shear test.
The hardening model used is the one proposed by Teodosiu [8] that is a physically-based microstructural model. It introduces internal variables taking into account the directional strength of dislocation structures and their polarity to describe both isotropic and kinematic hardening. For the present, only the comparison between kinematic, isotropic and mixed hardening will be considered. The influence of the polarity will be neglected to avoid intrusions between the two kinds of hardening. About the yield locus, three types of model can be used: Von-Mises or Hill surface to take into account the material anisotropy and texture-based models (discrete points of the yield locus are computed from the Taylor's model). In this paper, we use Hill yield locus. The laws described above have been implemented in the Finite Element code *lagamine* developed by M&S department at University of Liège. It is a non-linear large deformations code for solid mechanics.
A brief description of the model is proposed in section 2. In section 3 the choose of the different parameter values is explained and a description of the test performed is proposed. The goal of these tests is to give a first idea: in one hand of the effect of the different hardening, on the other hand of the behaviour of the numerical simulation.

2 CONSTITUTIVE MODEL

2.1 Description of the model

The model depicted hereafter has been developped by Teodosiu and Hu [8]. It takes into account the intregranular heterogeneity of the microstructure due to the evolution of dislocation structures, in addition to the isotropic and non linear kinematic hardening. This model is here depicted for the anisotropic Hill yield locus but it adapts to other ones. It depends on four state variables :

$$\underline{P},\ \underline{S},\ \underline{X},\ R \tag{1}$$

where $\underline{P}$ depicts the polarity, $\underline{\underline{S}}$ the evolution of the dislocation structures, $\underline{X}$ is the back stress and R the isotropic hardening. These state variables evolve as following, depending on the equivalent plastic strain rate $\dot{\bar{\varepsilon}}^p$:

$$\begin{aligned}
\dot{R} &= C_R\,(R_{sat} - R)\,\dot{\bar{\varepsilon}}^p \\
\underline{\dot{P}} &= C_p\,(\underline{N}_{\dot{\varepsilon}^p} - \underline{P})\,\dot{\bar{\varepsilon}}^p \\
\underline{\dot{X}} &= C_X \left(X_{sat}\,\frac{\underline{\sigma}' - \underline{X}}{\bar{\sigma}} - \underline{X} \right) \dot{\bar{\varepsilon}}^p \\
\dot{S}_D &= C_{SD}\,(g(S_{sat} - S_D) - hS_D)\,\dot{\bar{\varepsilon}}^p \\
\underline{\underline{\dot{S}}}_L &= -C_{SL} \left(\frac{S_L}{S_D} \right)^{n_L} \underline{\underline{S}}_L\,\dot{\bar{\varepsilon}}^p
\end{aligned} \tag{2}$$

with $\underline{N}_{\dot{\varepsilon}^p}$ the plastic strain rate direction ($\underline{N}_{\dot{\varepsilon}^p} = \underline{\dot{\varepsilon}}^p / |\underline{\dot{\varepsilon}}^p|$), S_D the strength of the dislocation structure associated with the currently active slip systems whereas $\underline{\underline{S}}_L$ is related to the persistent dislocation structure ($S_L = |\underline{\underline{S}}_L|$).

$$\begin{aligned}
\underline{\underline{S}} &= S_D \underline{N}_{\dot{\varepsilon}^p} \otimes \underline{N}_{\dot{\varepsilon}^p} + \underline{\underline{S}}_L \\
X_{sat} &= X^0_{sat} + (1-m)\sqrt{S_D^2 + qS_L^2}
\end{aligned} \tag{3}$$

and

$$h = \frac{1}{2} \left[1 - \frac{\underline{X} : \underline{N}_{\dot{\varepsilon}^p}}{X_{sat}\,\dfrac{\underline{\sigma}' - \underline{X}}{\bar{\sigma}} : \underline{N}_{\dot{\varepsilon}^p}} \right] \tag{4}$$

$$g = \begin{cases} 1 - \dfrac{C_p}{C_{SD} + C_p} \left| \dfrac{S_D}{S_{sat}} - P_D \right| & \text{if} \quad P_D = \underline{P} : \underline{N}_{\dot{\varepsilon}^p} \geq 0 \\ (1 + P_D)^{n_p} \left[1 - \dfrac{C_p}{C_{SD} + C_p} \dfrac{S_D}{S_{sat}} \right] & \text{otherwise} \end{cases}$$

The yield equation is given by

$$F = \bar{\sigma} - \sigma_0 - R - m|\underline{\underline{S}}| = 0 \tag{5}$$

with

$$\bar{\sigma} = \sqrt{(\underline{\sigma}' - \underline{X}) : \underline{\underline{H}} : (\underline{\sigma}' - \underline{X})} \tag{6}$$

In the equations (5) and (6), σ_0 is the initial elastic limit and $\underline{\sigma}'$ is the deviatoric part of $\underline{\sigma}$, $\underline{X}$ being deviatoric from the evolution law (2a). The usual flow rule is

$$\underline{\dot{\varepsilon}}^p = \dot{\lambda}\frac{\partial F}{\partial \underline{\sigma}} = \dot{\lambda}\frac{\underline{\underline{H}} : (\underline{\sigma}' - \underline{X})}{\overline{\sigma}} \tag{7}$$

with $\dot{\overline{\varepsilon}}^p = \sqrt{\underline{\dot{\varepsilon}}^p : \underline{\underline{B}} : \underline{\dot{\varepsilon}}^p}$ to get $\dot{\lambda} = \dot{\overline{\varepsilon}}^p$. In fact in the case of Hill criteria, $\underline{\underline{H}}$ is not reversible and $\underline{\underline{B}} \neq \underline{\underline{H}}^{-1}$. However, working in the five order deviatoric space, it is possible to build a pseudo reverse matrix $\underline{\underline{B}}$. Thanks to this choice of the equivalent plastic strain rate, the following energy relation (8) is fulfilled. Indeed, the dissipation power is

$$(\underline{\sigma}' - \underline{X}) : \underline{\dot{\varepsilon}}^p = (\underline{\sigma}' - \underline{X})\ \dot{\lambda}\ \frac{\underline{\underline{L}} : (\underline{\sigma}' - \underline{X})}{\overline{\sigma}} = \overline{\sigma}\dot{\lambda} = \overline{\sigma}\,\dot{\overline{\varepsilon}}^p \tag{8}$$

For this model, 13 material parameters must be identified R_{sat}, C_R, X^0_{sat}, S_{sat}, C_p, C_{SD}, C_{SL}, C_X, m, n_p, q and n_L. Note that an alternative to the formulation (2) of the kinematic hardening is the one proposed by Armstrong and Frederick (see [1] for example):

$$\dot{\underline{X}} = C(s\underline{\dot{\varepsilon}}^p - \underline{X}\,\dot{\overline{\varepsilon}}^p) \tag{9}$$

where C is the kinematic hardening parameter speed and s the saturation parameter. The two formulations differ by the direction of the back stress speed but the last one will not be investigated in this paper.
In the code *lagamine*, the integration of the constitutive law is achieved in a local frame [11] . Stress tensor is turned to this local frame at the beginning of each step of the non linear process and turned back to the global frame at the end of the step. The internal parameters are always expressed in this frame such that no Jauman correctors need to be added.

2.2 Hardening Laws selection

In view to split kinematic and isotropic hardening, the influence of the evolution of the dislocation structures matrix $\underline{\underline{S}}$ is not taken into account by setting $C_{SD} = C_{SL} = 0$. Fictitious steel parameters are assumed, $C_X = 10$, $X_{Sat} = 100MPa$ and $C_R = 10$, $R_{sat} = 200MPa$ for mixed hardening. The reminding hardening parameters needed in the computation are $m = 1$ and $\sigma_0 = 126MPa$ while the other are not used (C_p, n_p, n_L and q). The elastic behaviour of the high strength steel is assumed to be isotropic: $E = 209880MPa$, $\nu = 0.28$. For anisotropic Hill's parameter we use $F = 0.380365$, $G = 0.413445$, $H = 0.586555$ and $N = L = M = 1.414855$.
In the cyclic test, the load is broken up into three phases : the phase 1 is the monotonic loading, the phase 2 corresponds to the reverse loading and the phase 3 leads back to the end of the phase 1. This cyclic test is initially performed for a single element, for which we impose exactly the simple shear strain in the plan of the sheet. True stress/true

strain in global axes are depicted figure 1 below. The hardening parameters values are chosen such that the saturation is not reached at the end of the monotonic loading (here 10% strain). The "single" kinematic or isotropic hardening parameters have been fitted on the monotonic loading obtained for mixed hardening. We get respectively $C_R = 0$, $C_X = 10.1405$, $X_{Sat} = 295.5413MPa$ for single kinematic and $C_X = 0$, $C_R = 10.1405$, $R_{sat} = 295.5413MPa$ for single isotropic.

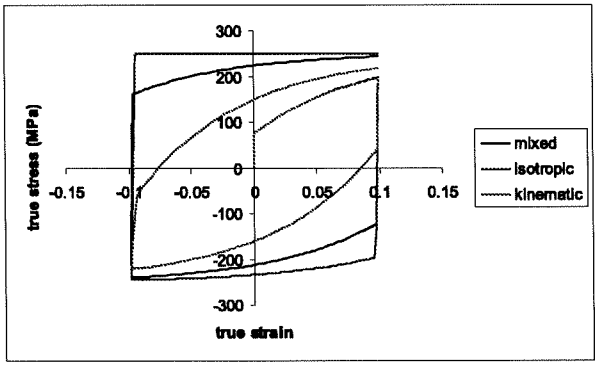

Figure 1: Hardening in simple shear test - $\sigma_{xy}/\varepsilon_{xy}$ in global axes - for a single 3D isoparametric element

In the case of kinematic hardening the slopes are different from the end of the previous phase to the beginning of a new one. Indeed, equation (2) shows that $\dot{\underline{X}}$ depends on $\underline{\sigma} - \underline{X}$. For a unidimensional problem in the shear direction, it means that if X is the same, σ changes from $\sigma_1 = \sigma_0 + X$ (ie $\sigma_1 - X = \sigma_0$) at the end of the phase 1 to $\sigma_2 = \sigma_1 - 2\sigma_0 = X - \sigma_0$ (ie $\sigma_2 - X = -\sigma_0$) at the beginning of the phase 2. Using the equation (2) with $\overline{\sigma} = \sigma_0$ we get $\partial X/\partial\overline{\varepsilon}^p = C_X(X_{Sat} - X)$ at the end of the phase 1 while $\partial X/\partial\overline{\varepsilon}^p = C_X(-X_{Sat} - X)$ at the end of the phase 2. This phenomena does not appear in the case of isotropic hardening since $\dot{R}$ depends only on R.

3 FEM simulation

In this section, we modelise the cyclic shear test of a steel sheet. The dimensions of the sample are respectively 30 mm for the length, 3 mm for the width and 1 mm for the thickness. The sheet is 3D meshed as shown on figure 2, x being the rolling direction and y the transverse direction. Only 0.5mm in the thickness is meshed because of symmetry. One face xz is jammed while on the opposite, y displacements are blocked and x displacements are imposed. We use an isoparametric, 8 nodes, 1 integration point element. The computation is not trivial to perform because of strain localization and hour glass deformation. This is why the mesh is not structured. Like in the previous section, loading is split in three phases. We present on the figure 3, σ_{xy} stress component at the end of the cycle, for a 3mm displacement.

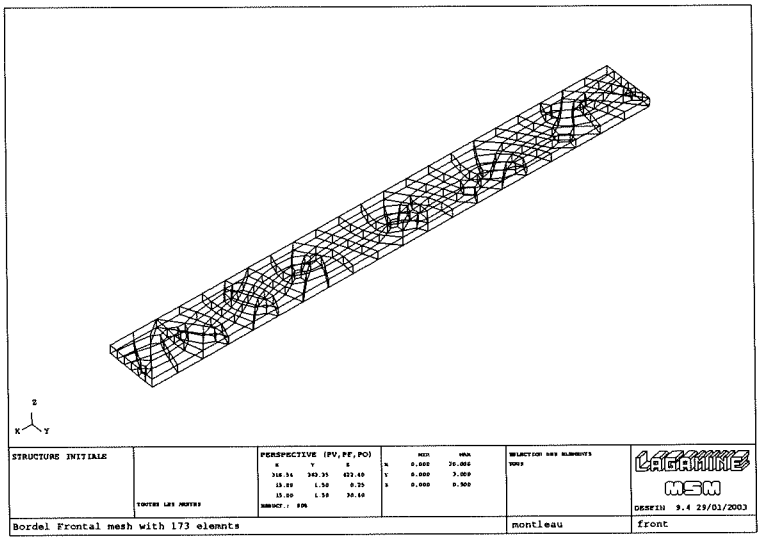

Figure 2: 3D mesh for a sheet

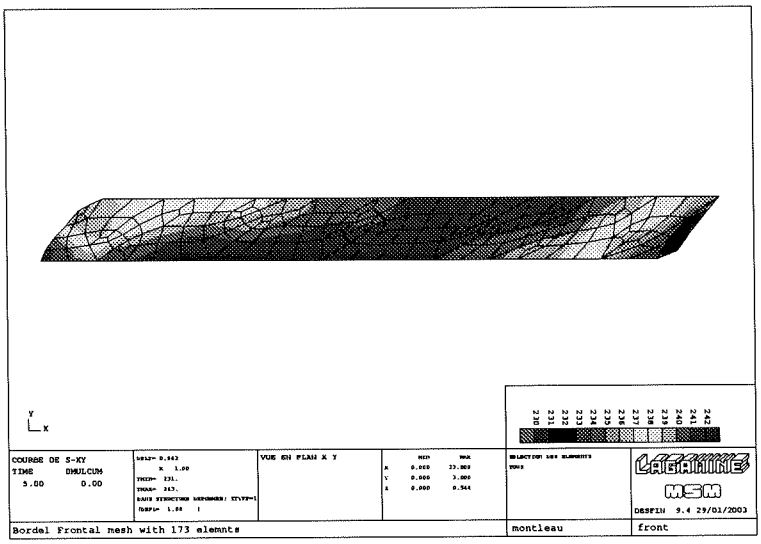

Figure 3: shear stress σ_{xy} in the deformed mesh at the end of a cycle

Two cases are studied: in the first one a $1mm$ displacement is imposed to avoid saturation ($\varepsilon_{xy\,max} = 0.12$) and in the second one a $3mm$ displacement ($\varepsilon_{xy\,max} = 0.43$) is imposed, which is the width of the sample. For both, cyclic test is performed for the three sets of parameters. For each of them, we exhibit the force with respect to the displacement in the figures 4a and 5a. Moreover we extract mechanical values from an element chosen in the center of the sheet. We exhibit true strain-true stress curves on the figures 5b and 5b.

These results show clearly the behaviour of the kinematic hardening (Baushinger ef-

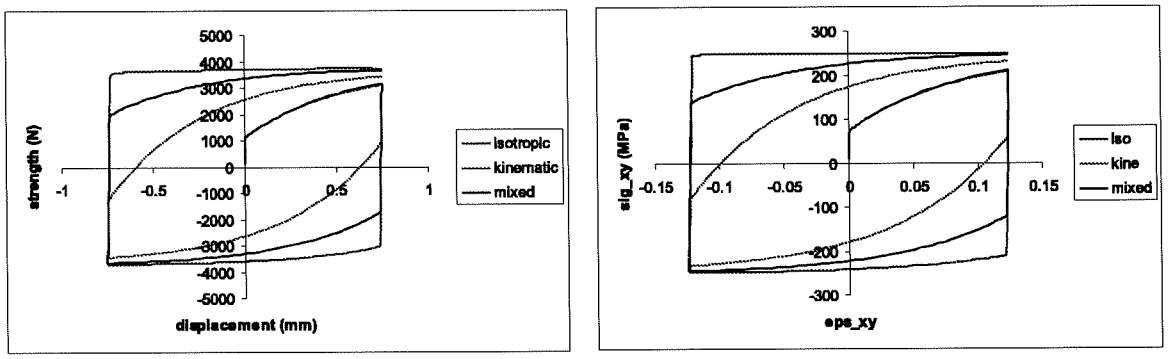

Figure 4: displacement 1mm a. force/displacement b. true stress/true strain in the heart of the sample

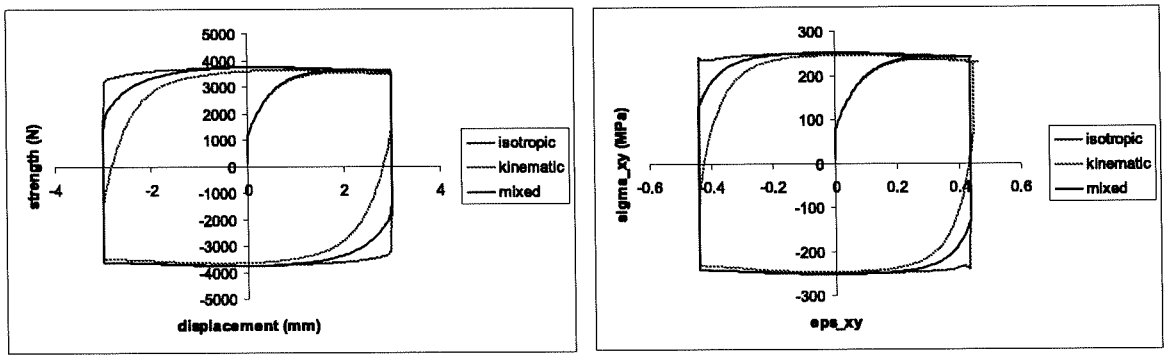

Figure 5: displacement 3mm a. force/displacement b. true stress/true strain in the heart of the sample

fect) and of the isotropic one. In the case where saturation is attempted before the end of the monotonic loading (figure 5), the two hardenings have only effects in a reduced area, when the material goes in plasticity at the beginning of the different phases. This shows that the reverse phase is compulsory to determine the set of parameters C_X, X_{Sat}, C_R and R_{Sat}.

A light softening is observed at then end of the different phases in figures 5. However, the plastic limit $\sigma_0 + r$ reaches saturation without softening. More investigation will be performed to well understand this behaviour.

From an experimental standpoint, this simulation exhibits a large homogeneous deformation zone and a force/displacement curve having the same shape as the strain/stress one, which shows that the edge effects has a negligible influence.

4 CONCLUSION

In this article, we have shown a simulation of an ordinary test where the most simple hardening parameters where studied. In future, more complicated tests(orthogonal test

and simultaneous shear plane strain test) will be simulated and compared with more elaborated hardening laws and yield locus descriptions. The final goal is a good knowledge of the different models in view to apply inverse method efficiently.

Aknowledgements

As Senior Research Associate of National Fund for Scientific Research, AM Habraken thanks this Belgian research fund for its support. This work has been performed in the programme "Ples d'attraction interuniversitaires" granted by Belgian state.

REFERENCES

[1] Khan, S., Huang S.: Continuum theory of Plasticity. J. Whiley & Sons, Inc (1995).

[2] Harbraken, A-M.: Contribution to constitutive laws of metals: micro-macro and damage models. Thesis (2001).

[3] Arnold, G., Hubert, O., Billardon, R.: Identification of kinematic and isotropic hardenings using a pure bending test machine. The 5th International Esaform, 2002, pp. 507-510.

[4] Weyler, R., Duffett, G., de la Cruz, C.: Effect of material hardening on springback problems in sheet metal forming . The 5th International Esaform, 2002, pp. 527-530.

[5] Bouvier, S., Haddadi, H.: Modelling the behaviour of a bake-hardening steel using a dislocation structure based model. The 4th International Esaform, 2002, pp. 429-432.

[6] Reis, A., Santos, A.D., Ferreira Duarte J., Rocha A.B., Say-Yi Li, Horfelin, E., Van Bael A., Van Houtte, P., Teodosiu, C.: Experimental validation of a new plasticity model of texture and strain-induced anisotropy. The 4th International Esaform, 2002, pp. 433-436.

[7] Lemaitre, J., Chaboche, J-L.: Mcanique des Matriaux solides. Dunod, 2e dition, 2001, pp. 163-251.

[8] Teodosiu, J., Hu, Z.: Evolution of the intergranular microstructure at moderate and large strains: modelling and computational significance. in Simulation of material processing: theory, methods and application (Proc. NUMIFORM' 95) ed. S.F Shen and P.R. Dawson, Balkema, Rotterdam, pp. 173-182.

[9] Duchêne, L.: Rapport de programmation de la loi Hill3D. Octobre 2001.

[10] Bouvier, S., Teodosiu C., Haddadi H., Tabacaru V.: Anisotropic Work-Hardening Behaviour of Structural Steels and Aluminium Alloys at Large Strains. EMMC6 Lige 2002, pp. 329-336.

[11] Munhoven, S.: Velocity gradients and local axes in three-dimensional finite element simulations. M.S.M Internal Report N 219, April 1995.

[12] Rauch, E. F.: Plastic anisotropy of sheet metals determined by simple shear tests. Material Science and Engineering A241 1998, pp. 179-183.

[13] Pijlman, H.H.: Sheet material characterization by multi-axial experiments. Doctoral Thesis presented at the University of Twente, The Neederlands 2001.